# Influence of cetyltrimethylammonium bromide and hydroxide ions on the interfacial tension and stability of emulsions of dodecane in aqueous silicate solutions

Matthieu Bertin, Donatien Gomes Rodrigues, Christel Pierlot, Cyrille Albert-Mercier, Catherine Davy, David Lambertin, Véronique Rataj

# Influence of cetyltrimethylammonium bromide and hydroxide ions on the interfacial tension and stability of emulsions of dodecane in aqueous silicate solutions

Matthieu BERTIN*[a], Donatien GOMES RODRIGUES[a], Christel PIERLOT*[b], Cyrille ALBER-MERCIER[c], Catherine DAVY[b], David LAMBERTIN[a] and Véronique NARDELLO-RATAJ[b]

[a]CEA, DES, ISEC, DE2D, SEAD, LCBC, Univ. Montpellier, Marcoule, France.

[b]Centrale Lille, Université de Lille, CNRS, Université Artois, UMR 8181-UCCS-Unité de catalyse et chimie du solide, Lille, France.

[c]LMCPA, Université de Valenciennes, Maubeuge, France.

*corresponding authors

Email: bertin.matthieu3@gmail.com, christel.pierlot@univ-lille.fr

## Abstract

Ensuring the synthesized material is optimized for the intended application requires an understanding of the emulsification mechanisms during synthesis. In concentrated sodium silicate solutions, we assume that silicate oligomers could stabilize the emulsion by positioning themselves at the interface. Moreover, the addition of an alkyltrimethylammonium which can interacted with the silicate oligomers should favour their positioning at the interface to increase the stability of the emulsion by Pickering effect. We studied the influence of sodium silicate and hydroxide concentrations with up to 6 $mol.L^{-1}$ (NaOH and $SiO_2$) on the interfacial tension ($\gamma$) between dodecane and water. Moreover, the effect of hexadecyltrimethylammonium bromide and decyltrimethylammonium bromide on the interfacial tension and the stability of the emulsion were studied. Adding the surfactant CTAB leads to partial precipitation but significantly decreases the interfacial tension to less than 4 $mN.m^{-1}$, effects that are not observed with DeTAB. The precipitate corresponds to CTAB-silicate and seems to contribute to the stabilization of the water/dodecane system, presumably through the Pickering effect. Moreover, works highlights that emulsion stability can be linked to the condensation/decondensation state of silicate species.

**Keywords:** silicate, emulsion, dodecane, tensiometry, SWAXS

# Introduction

Alkali silicate solutions can be used as reagents to produce silicate- and aluminosilicate-based materials. As ceramics, with binders such as geopolymers, they have found applications in construction [1,2] and as zeolites, they are widely used for sorption and catalysis [3–5]. Recent progress in the field of emulsion templating has further broadened their fields of application. Emulsion templating is an emerging method for the preparation of porous and composite materials [6,7], which allows the porous structure of a material to be adjusted via the nature and the volume fraction of the dispersed phase [8]. Controlling the volume fraction is key to producing a closed cell porous material as a percolated network is obtained when the volume fraction is higher than the packing fraction. Mesoporous materials [7,9] or hierarchically meso/macroporous monoliths [10,11] can be prepared by varying the initial mix. Open and closed-cell materials have different applications. The major applications of percolated porous materials are in catalysis and catalysis support [12], sorption [13] and separation [14–16], while closed cell porous materials are used for insulation and the solidification/stabilization of waste [17,18]. This study focusses on the use of emulsion templating for the immobilization of liquid organic nuclear waste, such as mixtures of dodecane and tributylphosphate. For these effluents, Portland cement-based binders cannot be used in the emulsion process because the organic compounds inhibit the hydration reactions of the clinker phases [19]. The emulsion technique can nonetheless be used with alkali-activated materials and geopolymers.

Alkanes are difficult to incorporate into alkaline silicate solutions in the absence of a surfactant. The most promising of the compounds tested in this context seem to be alkyl quaternary ammonium salts, with cetyltrimethyl ammonium bromide (CTAB) being particularly effective at reducing the interfacial tension between water and oil [17,18,20]. While many data are available on the interfacial tension between alkanes and aqueous solutions (i.e. water, or water with a low ionic strength, with and without surfactant) [21], only few have been published for concentrated solutions (concentration $\geq$ 1 mol.L$^{-1}$) such as those used for geopolymer synthesis. Furthermore, the bulk of these values come from studies of concentrated sodium and potassium hydroxides [20,22–29] and the literature on the variation of surface and interfacial tensions in the presence of alkali silicates is particularly sparse [30–33].

By combining tensiometry and small- and wide-angle X-ray scattering (SWAXS), the aim of this study was to understand the mechanisms governing the emulsion stability of an organic

liquid in a fresh geopolymer. In a first step, the concentration of silicate oligomers, the Si/Na molar ratio and the presence of a cationic surfactant were studied in terms of their effect on the oil/water interfacial tension. Dodecane was chosen as a model oil [20], and as surfactants, CTAB was compared with decyltrimethylammonium bromide (DeTAB) to examine the effect of the alkyl chain length. The different silicate oligomers produced by dissolving silica ($SiO_2$) in sodium hydroxide solutions were analyzed by SWAXS. In the second stage of the study, dodecane emulsions were prepared with different activation solutions and their stabilities were compared based on the hypothesis that the silicate solutions that minimized the interfacial tension would yield the most stable emulsions.

# 1. Materials and methods

## *1.1 Chemicals*

Tixosil 331 amorphous silica ($SiO_2$) was provided by Solvay with a purity of 97 %. Sodium hydroxide pellets (NaOH) were purchased from VWR. CTAB (97% purity) and DeTAB (99% purity) were purchased from Merck and Acros Organics respectively. Dodecane was provided by VWR, with a purity of 99%. Each chemical was used as received without further purification. Solutions were prepared using water deionized to a resistivity ≥ 18.2 MΩ·cm using a Milli-Q purification system.

## *1.2 Sample preparation*

### *1.2.1 Silicate solutions*

Sodium silicate solutions were prepared by dissolving amorphous silica (Tixosil 331) in sodium hydroxide solutions (prepared with water degassed under a stream of argon for 1 h to avoid carbonation of the solution) at the desired concentration. The solutions were stirred for 24 h and then centrifuged at 4500 rpm for 20 min to remove the small particles produced by silica impurities. All solutions were kept sealed to minimize atmospheric carbonation. Since the solutions were basic, the $SiO_2$ was assumed to be fully dissolved. The silicate solutions were characterized by their concentrations of $SiO_2$ and NaOH and the corresponding Si/Na molar ratio.

### *1.2.2 Separation of precipitates obtained by adding CTAB ($10^{-2}$ mol.L−1) to the activated solution (Si/Na=0.75 and [NaOH] = 6 mol.L−1).*

CTAB (364 mg) was added to 10 mL of the sodium silicate solution with Si/Na = 0.75, obtained by dissolving $SiO_2$ ([$SiO_2$] = 4.5 mol.$L^{-1}$) in a 6 mol.$L^{-1}$ solution of NaOH, as described above. The solution was stirred for 1 h and then filtered through a Büchner funnel with a 0.45 μm filter. The precipitate was recovered and dried in an oven at 60 °C for three days.

## *1.3 Interfacial tensions*

Interfacial tensions were measured using a Tracker pendant-drop tensiometer (Teclis Scientific). The aqueous phase was placed inside a glass cell and dodecane was loaded into a syringe. The J-shaped needle was immersed in the aqueous phase in the cell so that the shape of the droplet produced could be analyzed. A minimum of three measurements were performed for each solution.

## *1.4 Small- and wide-angle X-ray scattering (SWAXS)*

SWAXS measurements were performed on a Xenocs bench using Mo radiation (λ = 0.71 Å). The X-ray beam was collimated with a focusing multilayer mirror and two pairs of scatterless slits. The X-rays were then scattered by the sample placed in 2 mm diameter glass capillaries. The maximum time between sample preparation and analysis was limited to 6h so that capillary degradation was negligible. The scattered beam was recorded using a large 2D detector (MAR Research 345) located about 75 cm downstream of the sample. It was calibrated using silver behenate powder. The averaged signal obtained from the FIT2D software was plotted versus the magnitude of the scattering vector, q, calculated as follows,

$$q = \frac{4\pi}{\lambda}\sin\left(\frac{\theta}{2}\right) \quad (1)$$

where λ is the wavelength of the incident radiation and θ, the scattering angle. A large q-range (0.025 - 2.8 $Å^{-1}$) was covered thanks to off-center detection and the experimental resolution was $\Delta q/q = 0.02q/q = 0.02$. The typical exposure time for the silicate solutions was 3600 s. Usual corrections for background subtractions (from the empty cell and detector noise) were applied, and intensities were normalized using a high density polyethylene standard (Goodfellow) to obtain I(q) in $cm^{-1}$. The SWAXS data were finally analyzed by fitting a mathematical model using the software SASView (sasview.org).

Biphasic mixtures were prepared by mixing sodium silicate solutions with or without surfactant (7.5 mL, with defined concentrations of $SiO_2$ and NaOH), with dodecane (7.5 mL)

in a glass flask, followed by magnetic stirring for 4 h. The mixtures were then centrifuged at 4500 rpm for 10 min to separate the aqueous and solvent phases for SWAXS analysis.

### *1.5 1H Nuclear Magnetic Resonance*

$^{1}$H NMR spectra were recorded on a 300 MHz Bruker Avance spectrometer for mixtures prepared with deuterated solvents purchased from Eurisotop. Chemicals shifts were referenced to the residual water signal at 4.79 ppm.

### *1.6 Infrared spectroscopy*

Fourier transform infrared (FT-IR) spectra were recorded on a ThermoScientific iS50 Nicolet FT-IR spectrometer in attenuated total reflection (ATR) mode, using a thin film of the analyzed solution or solid, for wave numbers ranging from 400 to 4000 $cm^{-1}$ at a resolution of 1 $cm^{-1}$.

## 2. Results

### *2.1 Interfacial tension*

#### *2.1.1 Silicate-dodecane interfaces without surfactant*

The morphology and stability of dodecane droplets in emulsions depend strongly on the interfacial tension, namely the energy per unit area required to increase the interfacial area between the two immiscible phases, the organic phase and the silicate solution. The formulation of the fresh geopolymers can be adjusted by varying the concentrations of silica and soda depending on the desired final properties of the cured geopolymers (in terms of porosity for example, or compressive strength). To cover a large range of properties, we measured the interfacial tension of dodecane droplets in solutions containing 0–6 $mol.L^{-1}$ sodium hydroxide and Si/Na molar ratios of between 0 and 1.

**Figure 1A** shows the variation of the interfacial tension, $\gamma$ ($mN.m^{-1}$), between dodecane and aqueous sodium hydroxide as a function of the concentration of sodium ions. In neat water, the water-oil interfacial tension is 47 $mN.m^{-1}$, which is close to previously reported values of about 52 $mN.m^{-1}$ [21,34,35]. The difference can be accounted for in part by the different levels of purity of the dodecane, used either directly or after purification on silica columns

[36]. In aqueous sodium hydroxide (Si/Na = 0) γ first decreases to a minimum of about 32.5 $mN.m^{-1}$ at $[Na^+] = 1$ $mol.L^{-1}$, then slowly increases up to 36.5 $mN.m^{-1}$ at $[Na^+] = 6$ $mol.L^{-1}$.

With Si/Na = 0.75 (**Figure 1A),** the interfacial tension also decreases at first until $[Na^+] = 1$ $mol.L^{-1}$, before remaining constant at 28 $mN.m^{-1}$ up to $[Na^+] = 6$ $mol.L^{-1}$. The data for the solution with Si/Na = 1 follow the same trend, namely a strong decrease in γ up to $[Na^+] = 2$ $mol.L^{-1}$ ($\gamma = 23$ $mN.m^{-1}$), and then a slight further decrease until $[Na^+] = 6$ $mol.L^{-1}$ ($\gamma = 18$ $mN.m^{-1}$). As shown in **Figure 1B**, in 1 $mol.L^{-1}$ sodium hydroxide, γ remains approximately constant (≈ 30 $mN.m^{-1}$) whatever the silicate concentration (0 to 1 $mol.L^{-1}$). With $[Na^+] = 6$ $mol.L^{-1}$, γ decreases continuously (from 47 to 18 $mN.m^{-1}$) with the Si/Na ratio.

### *2.1.2 Sodium hydroxide solution-dodecane interfaces with CTAB and DeTAB surfactants*

**Figure 1C** shows how the interfacial tension evolves in sodium hydroxide solutions without silicates (Si/Na = 0), and with or without either DeTAB or CTAB at $10^{-3}$ and $10^{-2}$ $mol.L^{-1}$. The experiments for $[Na^+] = 0$ $mol.L^{-1}$ (where the Si/Na ratio is not defined) were performed in pure water (without or with surfactant).

As expected, the interfacial tension is lower in the samples with surfactants. With CTAB at $10^{-3}$ and $10^{-2}$ $mol.L^{-1}$, the alkalinity of the solution does not significantly affect the interfacial tension, which remains roughly constant at around 6 $mN.m^{-1}$ and 4 $mN.m^{-1}$, respectively. The measurements were stopped at 3 $mol \cdot L^{-1}$ for $[CTAB] = 10^{-2}$ $mol.L^{-1}$ and at 4 $mol.L^{-1}$ for $[CTAB] = 10^{-3}$ $mol.L^{-1}$ because the interfacial tensions were below the sensitivity limit of the technique. For DeTAB, the interfacial tension decreases as the alkalinity of the solution increases, before leveling off at $\gamma = 10$ $mN.m^{-1}$.

### *2.1.3 Dodecane interface with silicate solutions containing CTAB or DeTAB*

**Figure 1D** shows the evolution of the interfacial tension as a function of the $Na^+$ concentration in silicate solutions with a Si/Na molar ratio of 0.75, containing either DeTAB or CTAB. With CTAB, measurements at $[CTAB] > 10^{-4}$ $mol \cdot L^{-1}$ proved impossible because of the formation of a white precipitate. The interfacial tension first decreases from 21 to 11 $mN \cdot m^{-1}$ from 0 to 1 $mol.L^{-1}$ Na+, then gradually increases up to a value slightly higher than those measured without surfactant, indicating that CTAB's surfactant effect becomes progressively weaker as the sodium concentration increases.

With DeTAB, the solutions remained transparent. At a DeTAB concentration of $1.10^{-3}$ mol.L$^{-1}$, the interfacial tension slowly increases from 21 to 25 mN.m$^{-1}$ between 0 to 2 mol.L$^{-1}$ $Na^+$, then decreases and remains at about 9 mN.m$^{-1}$. For [DeTAB] = $10^{-2}$ mol.L$^{-1}$, the interfacial tension decreases from $\gamma$ = 23 to 8 mN.m$^{-1}$ in going from pure water to [$Na^+$] = 6 mol.L$^{-1}$.

## *2.2 Ammonium-silicate salt precipitation*

Previous studies have shown that to incorporate alkanes into geopolymer emulsion pastes, the CTAB concentration should be set to between $10^{-3}$ and $10^{-2}$ mol.L$^{-1}$ [20]. However, at $Na^+$ concentrations above 1 mol.L$^{-1}$ and Si/Na = 0.75, adding more than $10^{-3}$ mol.L$^{-1}$ CTAB leads to precipitation, presumably of a CTA-silicate salt. To confirm this, an aqueous silicate solution with [CTAB] = $10^{-2}$ mol.L$^{-1}$, [$Na^+$] = 6 mol.L$^{-1}$ and a Si/Na molar ratio of 0.75 was prepared and filtered to isolate the precipitate. After drying, the solid was analyzed by $^1$H NMR (**Figure 2a**) and FTIR (**Figure 2b**) and compared with the corresponding spectra of pure CTAB (see Supporting Information for details).

Based on Kreke *et al.*'s analysis [37], the $^1$H NMR spectra in **Figure 2a** confirm that the precipitate is a CTA-based compound. Furthermore, the signals from the hydrogens in the methyl group and in the α position on the nitrogen atom are distorted and are shifted from 3.10 to 3.15 ppm and from 3.31 to 3.36 ppm respectively. This change compared with pure CTAB in the chemical shifts of protons close to the quaternary ammonium group may be due to exchange of the $Br^-$ ion with more electronegative deprotonated silicate species.

In the FTIR spectra **(Figure 2b)**, the broad peak at around 3300 cm$^{-1}$ can be assigned to the O-H stretching vibrations of hydroxyls and water [38].The presence of ammonium in the precipitate can be deduced from the bands corresponding to the scissoring modes of $CH_2$-$N^+$ at 1439 and 1408 cm$^{-1}$. The band at 911 cm$^{-1}$ arises from the C-N bound in the trimethylamine head group while the bands at 2915 cm$^{-1}$, 2848 cm$^{-1}$, and 719 cm$^{-1}$ correspond respectively to C-H anti-symmetric stretching, $CH_2$ symmetric stretching, and $(CH_2)_n$, rocking modes in the aliphatic chain. The bands at 1101, 995 and 864 cm$^{-1}$ correspond to Si-O vibrations. This NMR and FT-IR analysis thus confirms that the precipitate is a cetyltrimethylammonium silicate salt [39–41].

## *2.3 Small angle X-ray scattering analysis*

The SWAXS spectra collected for different Si/Na ratios (0–1) to get an insight into the structures and sizes of the silicate oligomers in the alkali solutions are presented in **Figure 3a**

and **3b** for [NaOH] = 1 and 6 mol.L$^{-1}$, respectively. In these spectra, the broad peak at higher q-values and centered at 2.2 Å$^{-1}$ is typical of intermolecular O-O bonds in water molecules. The strong peak at q = 0.7 Å$^{-1}$ observed in the most concentrated sodium hydroxide solutions (6 mol.L$^{-1}$) is attributed to hydroxide correlation [42]. In the absence of silicates, the intensity decreases slightly at low q values (from 0.025 to 0.7 Å$^{-1}$) before leveling off at q ~ 0 Å–1. The scattering intensity of pure water is lower than that of the other solutions, at about 0.01 cm-1, a value that is related to the isothermal compressibility of water. In the presence of silicates, the scattering intensity increases at low scattering angles (q < 0.8 Å$^{-1}$), the more so the higher the silicate concentration is. This behavior is typical in the presence of silicate oligomers with a finite size and the plateau intensity is related to the volume fraction of scatterers. The higher the Si/Na ratio of the solution, the higher the I(0) value of the SAXS profile is, indicating that in agreement with the literature, the volume fraction of scattering entities (Φ) increases with the Si/Na ratio. For the solution with [$Na^+$] = 1 mol.L$^{-1}$ and Si/Na = 1, the slight increase in the scattering intensity at the lowest q values may be due to attractive interactions. Similarly, the hump observed at q = 0.5 Å$^{-1}$ at the highest Si/Na ratios with [$Na^+$] = 6 mol.L$^{-1}$ may be related to repulsive interactions between oligomers.

## *2.4 Dodecane/Silicate emulsions*

To investigate the impact of surfactants and sodium silicate on the stability of dodecane/water emulsions, dodecane and silicate solutions were mixed isovolumically. Each emulsion was prepared from a silicate solution. To focus on the effects of the surfactants, a first experiment was conducted with [NaOH] fixed at 6 mol.L$^{-1}$ with an Si/Na molar ratio of 0.75. The two components were dispersed using an Ultra-Turrax homogenizer at 13,500 rpm for 60 s to avoid the formation of submicronic dodecane droplets that can only be stabilized by Brownian motion. The use of different formulations revealed differences in the formation and the stability of the emulsions prepared with CTAB and DeTAB, and the presence or not of CTA-silicate particles in the aqueous phase. **Figure 4** lists the systems obtained at different times (30 s, 6 min and 60 min) after emulsification using the following formulations: (A) dodecane mixed with a pure silicate solution, (B) dodecane mixed with a silicate solution containing $10^{-2}$ mol.L$^{-1}$ CTAB, with the precipitate left in the aqueous solution, (C) dodecane mixed with a silicate solution containing $10^{-2}$ mol.L$^{-1}$ CTAB, with the precipitate filtered out of the aqueous solution, and (D) dodecane dispersed in a silicate solution containing $10^{-2}$ mol.L$^{-1}$ DeTAB.

In system **(A)**, the dodecane and the silicate solution were initially well mixed but rapidly separated. The photograph taken after 30 s shows a turbid phase at the bottom of the flask beneath the transparent upper phase. It is logical to suppose that the lower phase is a dispersion of dodecane droplets in the aqueous phase while the upper phase is the undispersed excess dodecane. This could not be confirmed however because the milky phase disappears rapidly, highlighting the instability of the dispersion. In systems **(B)** and **(D)**, prepared with CTAB and DeTAB respectively, surfactant-silicate salts precipitate as described in Section 2.2. With CTAB, the whole volume of the mixture is emulsified, but early in the ageing process, an aqueous solution is first released, followed by a dodecane rich phase. A greater volume of water is released than of oil, suggesting that the emulsion is of the water-in-oil type.

In contrast, the formulation with DeTAB leads to the formation of an oil-in-water emulsion at the bottom of the flask (after 30 s). The upper phase is the excess dodecane. Between 30 s and 60 min – i.e. during early aging of the dispersion – the emulsion separates into a concentrated phase at the interface of the aqueous and oily phases. Finally, comparing systems (B) and (C) shows that the CTAB-silicate species contribute to the emulsification of the solution and then stabilize the dispersion.

In a second stage, the influence of the Si/Na molar ratio was studied at two concentrations of NaOH (1 and 6 $mol.L^{-1}$). The emulsions were prepared using CTAB-based silicate solutions with various [NaOH] and Si/Na ratios. The concentration of CTAB in the silicate solution was fixed at $10^{-2}$ $mol.L^{-1}$ and the precipitate was left in the silicate solution. **Figure 5** shows photographs of the different emulsions after 60 and 120 min of ageing. Systems G and H destabilize more rapidly than systems E and F do, indicating that for the same Si/Na ratio, emulsions with higher NaOH concentrations are more unstable. It is also clear that at a given Si/Na ratio, the stable emulsion volume is lower and the destabilization kinetics faster in the emulsions with higher NaOH contents

# 3. Discussion

## *3.1 Silicate oligomer size*

A simple estimate of the size of silicate entities is the gyration radius ($R_g$) obtained using the Guinier approximation [39], expressed in linearized form as

$$\ln[I(q)] = \ln[I(0)] - \frac{q^2 R_g^2}{3} \quad (2)$$

where I(0) is the plateau scattering intensity, $R_g$ is the average gyration radius of the silicate units, and q is the magnitude of the scattering vector. The Guinier equation was fitted to the plateau regions of the experimental SWAXS data, with the parameters constrained to $qR_g \leq 1$ as is typically done. The gyration radius is plotted versus the Si/Na ratio in **Figure 6**. Because of attractive and/or repulsive interactions, the scattering intensity did not level off in the solutions with $[Na^+]$ = 1 mol.L$^{-1}$ and Si/Na = 1 and with $[Na^+]$ = 6 mol.L$^{-1}$ and Si/Na = 0.75 and 1 and these data were not analyzed using the Guinier model. **Figure 6** shows that the gyration radius decreases from 4.5 Å to 1.5 Å as the Si/Na ratio decreases from 0.75 to 0.1, regardless of the $Na^+$ concentration (1 or 6 mol.L$^{-1}$). The decrease in Rg reflects the decondensation of silicate species, as has already been observed with [Na+] = 1 mol.L$^{-1}$ by Dupuis et al. [43]. Our results indicate that this remains the case in more concentrated NaOH solutions (6 mol.L$^{-1}$). Extrapolating the data in **Figure 6**, the estimated $R_g$ (≈ 5 Å) for Si/Na = 1 is in agreement with the results of Dupuis et al. [43] ($R_g$ = 4.5 Å). These results along with $^{29}$Si NMR results in the literature [9,43,44], suggest that monomer $Q^0$ species predominate for Si/Na molar ratios ranging from 0.05 to 0.2 and that dimer $Q^1$ units are the major species at slightly higher Si/Na ratios [9,44,45]. Around Si/Na = 1, silicon is mainly present as $Q^2$ and $Q^3$ units and the silicate oligomers are trimers or tetramers at Si/Na molar ratios above 1. The $Q^i$ speciation is show as a function of the Si/Na ratio in **Figures 1B** and **4.** The influence of dodecane and CTAB ($10^{-4}$ mol.L$^{-1}$) on the interconnectivity of silicate groups was investigated by contacting the organic and aqueous phases and then separating them for SWAXS analysis. The results in both phases are similar to those obtained in the absence of surfactant (see supplementary information), indicating that neither dodecane nor CTAB alter the structural organization of these silicate solutions.

## *3.2. Interfacial tension*

### *3.2.1 Sodium hydroxide solution / dodecane*

**Figure 1a** shows how γ evolves with the sodium hydroxide concentration, with a minimum (32.5 mN.m$^{-1}$) at 1 mol.L$^{-1}$NaOH. The same trend has already been observed in crude oil with different minerals (NaOH, $Na_2CO_3$ and $NH_4OH$) and the organic alkaline compound diethylamine, and the minimum γ also occurred at an alkali concentration of about 1 mol.L$^{-1}$ [26]. Crude oils are known to contain acidic components such as naphtenic acids which, after

deprotonation by alkali species, act as surfactants, leading to γ values that are lower (less than 1 $mN.m^{-1}$) than in the present case. However, this minimum in γ has also been observed for crude oils without naphtenic acid [32] or with pure n-$C_{11}$, $C_{21}$, $C_{14}$ [46] and $C_{16}$ [29] alkanes. This clearly indicates that $HO^-$ anions reduce the interfacial tension independently from any carboxylate surfactants present in the oil.

The action of $HO^-$ groups on γ can be explained by the organization of water molecules at the water/air and water/oil interfaces [47]. In alkali solutions, strong hydrogen bonds between interfacial water and $HO^-$ ions lead to the specific adsorption of $HO^-$, which alters the surface tension, as shown by Kasmaee et al. [27]. Although these hydrogen bonds also exist in bulk water, it has been suggested [48] that in the bulk, a fraction are broken by Brownian motion. In other words, the more restricted movement of the water molecules in the interfacial layer may allow more persistent H bonding between $HO^-$ and water molecules. Even if the adsorption mechanism of the $HO^-$ anions themselves is far from clear, this would explain why in the present case the interfacial tension (35 $mN.m^{-1}$) in the 1 $mol.L^{-1}$ NaOH solution is lower than in neat water (47.5 $mN.m^{-1}$).

The interfacial tension can also be affected by changes in $Na^+$ hydration, but in these solutions, since the $Na^+$ ions tend to remain fully hydrated in the bulk rather than partially hydrated at the interface [22], the influence of $Na^+$ ions is likely to be insignificant and the variations in γ that occur with changes in the NaOH concentration should be attributed mainly to the behavior of the $HO^-$ ions.

### *3.2.2 Sodium silicate solution /dodecane*

It is known that sodium silicates obtained by dissolving sodium orthosilicate $Na_4SiO_4$ [30] or sodium metasilicate $Na_2SiO_3$ [31] or by varying the Si/Na ratio [32,33] decrease the interfacial tension between water and crude oil, and sodium silicates have thus already been studied in enhanced oil recovery (EOR) processes. Although sodium silicates are a complex family of compounds, changing the Si/Na ratio allows them to be tailored for specific EOR applications (sequestering, water wetting, permeation, and γ-reduction). The properties required in each case depend on the size, charge, and basicity of the silicate molecules, which can be adjusted by changing the Si/Na ratio and concentration [32]. For example, a number of silicates with different Si/Na ratios (0.25, 0.6 and 0.8) have been shown to be equivalent to NaOH in their ability to reduce the interfacial tension between crude oil and water.

**Figure 7** shows the different silicon $Q^n$ species. It is generally accepted that at Si/Na molar ratios lower than 1.5, $Q^0$, $Q^1$, $Q^2$ and $Q^3$ groups can be found in 18 distinct oligomers, the largest of these chains containing eight silicon group [49]. Although the precise distribution of chain lengths under the different experimental conditions studied here is difficult to determine, some general trends can be identified as a function of the Si/Na ratio.

The presence of $HO^-$ ions in solution, leads to the breaking of some Si-O-Si bons, with the negative charge either transferred to the SiO unit (**Eq. 4**) or remaining on the $HO^-$ group (**Eq. 5**). In both cases, adding silica to the solution consumes $HO^-$ and leads to the creation of $SiO^-$ units. Thus for all concentrations of NaOH between 0.05 and 6 $mol.L^{-1}$, the $HO^-$ concentration is lower in the solutions with Si/Na = 0.75 than in the pure NaOH solutions (Si/Na = 0). This is correlated with a drop of 10 $mN.m^{-1}$ in the interfacial tension, (**Figures 1C** and **1D**), clearly indicating that the silicate groups themselves have an interfacial tension reducing effect.

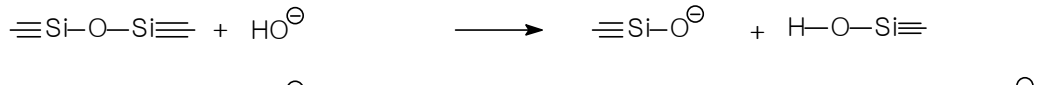


(4)

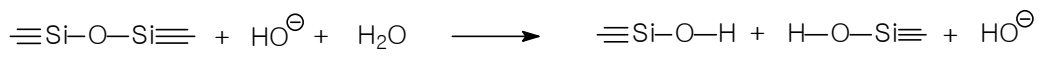


(5)

Solid $SiO_2$ enters the solution state as $Q^0$ monomers when hydrolyzed with sodium hydroxide [50]. Silicate oligomers thus form via the combination of smaller fragments in solution, with populations of higher order oligomers reaching detectable levels only when the total silicon concentration exceeds certain thresholds. The relative population of individual species is a steeply declining function of the silicon chain length, and the most probable oligomers are those that can be formed by bimolecular reactions of the predominant lower-order structures, such as monomers, dimers, trimers etc. In therefore seems logical to consider candidate assignments in order of increasing chain length, with increasing Si/Na ratios.

According to the literature [43,44], silicon is mainly present as $Q^0$ monomers at Si/Na molar ratios between 0.05 and 0.2; $Q^1$ dimers then predominate for Si/Na ratios up to 0.5 while at higher Si/Na ratios, the majority of silicon groups are $Q^2$ and $Q^3$ units, but it is not clear which of the two predominate. The fact that $\gamma$ decreases as the Si/Na ratio increases (**Figure 1a**) indicates that $Q^0$ monomers, $Q^1$ dimers and silicon chains with $Q^2$ and $Q^3$ groups all decrease the interfacial tension with trimers and larger oligomers having the strongest effect.

### *3.2.3 Critical micellar concentration of CTAB and DeTAB and precipitation of CTAB-Silicate salts*

Adding salt strongly decreases the critical micellar concentration (CMC) of ionic surfactants mainly because the counter ions screen the surface charges of the aggregates. Above the CMC, surfactants form micelles of different sizes and shapes, the solution remaining clear if the micelles are fully soluble or becoming turbid if they are only partially soluble. **Figures 1C** and **1D** show that in the absence of $Na^+$ ions, γ decreases to a minimum value of 5 $mN.m^{-1}$ at a CTAB concentration slightly above $10^{-3}$ $mol.L^{-1}$. This in consistent with the CMC of CTAB at 25°C, $9 \times 10^{-4}$ $mol.L^{-1}$ [51–53]. Because its alkyl chain is shorter, DeTAB has a higher CMC ($7.2\ 10^{-2}$ $mol.L^{-1}$) [54] and has less of an effect on γ, which only decreases to a minimum of about 20-24 $mN.m^{-1}$. Adding up to 3 $mol.L^{-1}$ $HO^-$ in the CTAB solutions does not significantly affect γ, but above 3 or 4 $mmol.L^{-1}$ $Na^+$ (depending on the CTAB concentration) the interfacial tension becomes too small to measure (γ <4 $mN.m^{-1}$). In parallel, the CMC of CTAB decreases as the $HO^-$ concentration increases, with a factor ten difference between the CMC in water (CMC = 8 $mmol.L^{-1}$) and in 0.5 $mol.L^{-1}$ NaOH (CMC = 0.7 $mmol.L^{-1}$) [27], but the micelles remain water soluble. Adding sodium silicate (**Figure 1D**) leads to the precipitation of CTAB and the turbidity of the solution precluded further interfacial tension measurements. The fact that no such clouding was observed in the pure NaOH solution (without surfactant) shows that this is due to interactions between CTAB and silicate species. Note also that there was no precipitation in the solution with the lowest CTAB concentration ($10^{-4}$ $mol.L^{-1}$, **Figure 1D**). This lowering effect of silicate anions on the CMC of CTAB has been reported previously [55], and is in agreement with the reported high binding affinity of silicate ions to CTAB micelles [40,41,56]. Thus, adding silicates to solutions containing CTAB, even at low concentration, leads to the fusion of small spherical micelles into elongated rod-like rigid micelles [39,40] that are poorly soluble in water. Silicate aggregates with DeTAB (which has a higher CMC of $7.2\ 10^{-2}$ $mol.L^{-1}$) [54] are less compact and larger than those that form with the more strongly binding CTAB [57]. This is reflected in **Figures 1C** and **1D**, where γ follows the same trend in the solutions with DeTAB at $10^{-3}$ and $10^{-2}$ $mol.L^{-1}$ as in those without surfactant, both in the absence (**Figure 1C**) and in the presence of silicates with Si/Na = 0.75 (**Figure 1D**).

## *3.3 Stability of emulsions of dodecane and aqueous silicate*

### *3.3.1 Positive effect of $HO^-$*

Studies of the pH dependence of zeta potentials and of ionic strength effects have shown that $HO^-$ anions adsorb at water/oil interfaces [36,58,59]. The zeta potential (ζ) of several alkanes (octane, decane and dodecane) has a sigmoidal pH dependence characterized by an isoelectric point at pH = 2-3, a half adsorption point at about pH = 5.5, and a minimum value (ζ = -85 mV) above pH 9. More generally, the fact that water/oil interfaces are often negatively charged even in the absence of any surfactant has been attributed to $HO^-$ being absorbed more strongly than other charged species are [60]. Moreover, very stable oil/water emulsion can be produced in the absence of surfactant provided the pH is sufficiently high and the droplets sufficiently small. For example as shown by Beattie et al. [58], a homogenized 2% solution of hexadecane in water at pH = 9-10 without surfactant produces small submicrometer droplets with a very negative zeta potential (ζ = -120 mV) and the emulsion remains stable for days. In general, hydroxide-stabilized emulsions can be produced with oils that are poorly soluble in water [58]. Note that while the presence of sodium hydroxide and sodium silicate makes the mixtures used to incorporate alkanes into geopolymer suspensions very basic, the surface charge generated on the surface of the oil droplets is insufficient to stabilize an emulsion, which is why CTAB is often added to activating solutions [20]**.**

### *3.3.2 Dual stabilizing effect of CTAB in silicate solution/dodecane emulsions*

The data presented in **Figure 4** highlight the role of CTAB in the stabilization of emulsions of silicate solution (Si/Na = 0.75 and $[Na^+]$ = 6 $mol.L^{-1}$) and dodecane. Without surfactant, the interfacial tension is 25.9 $mN.m^{-1}$ (**Figure 1D**) and the suspension separates into two phases within 30 s. Adding $10^{-2}$ $mol.L^{-1}$ DeTAB lowers γ (to 8.1 $mN/m^{-1}$) but the emulsion is not stable and the mixture tends rapidly to a creamed system at equilibrium. However, the fact that the aqueous phase at the bottom of the flask is turbid highlights the presence of oil droplets in the water phase and shows that DeTAB nonetheless has a small stabilizing effect and confirms its hydrophilic behavior [61]. As mentioned above, adding $10^{-2}$ $mol.L^{-1}$ CTAB to the silicate solution leads both to a strong decrease in γ (< 4 $mN/m^{-1}$) and to the precipitation of a white CTA-silicate solid. The CTAB based emulsion remains homogenous for 30 s and is more stable than the DeTAB system.

After 6 and 60 min, the creaming observed is characteristic of water-in-oil emulsions, proving that CTAB behaves hydrophobically in the aqueous phase. However, the low γ value induced

by $10^{-2}$ mol.$L^{-1}$ CTAB is not the only reason this emulsion is more stable since after filtration, the aqueous phase produces an unstable dispersion of droplets when stirred with dodecane. This means that the CTA-silicate based precipitates (partially water soluble micelles) must also have a stabilization effect on the emulsion, possibly through the Pickering effect at the oil/water interface [62].

### *3.3.3 Stabilizing effects of both the Si/Na ratio and the size of the silicate oligomers*

The results presented in section 2.1.1 show that γ decreases as the Si/Na ratio increases, while **Figure 5** shows that for all sodium concentrations, the most stable emulsions in the presence of CTAB are those with the lowest Si/Na ratio.

In producing a stable emulsion in these systems therefore, reductions in γ have to be balanced against the degree of polymerization of the silicate species. Although the most stable emulsions are generally obtained when the interfacial tension is lowest; here, the most stable emulsions were those with intermediate γ values. Indeed, the results indicate that the interfacial tension has to be reduced but that the conditions at which γ is lowest are not optimal for stabilizing the biphasic system. This is because the silicate species also play a role in emulsion formation. The silicates are predominantly monomers ($Q^0$) at low Si/Na ratios and mostly oligomers ($Q^2$ and $Q^3$) at the highest Si/Na ratios, with the SWAXS analysis showing that the higher the Si/Na ratio is, the larger the oligomers are.

The comparison between systems in **Figure 4** provides hints about how the emulsions are stabilized and reveals a possible role of silicate monomers. The data show that the CTA-silicate species are important in stabilizing the emulsions. **Figure 5** completes this information by demonstrating the importance of the nature of the silicate species (monomer versus larger oligomers). Moreover, the nature of the $CTA^+$-based precipitates depends on the nature of the silicate units and given the steric hindrance of the trimethylammonium group – $N(Me)_3^+$, this suggests that CTA interacts preferentially with silicate monomers rather than oligomers. This could be confirmed by determining the $Q^i$ composition of the CTA-silicates using $Si^{29}$ NMR.

Furthermore, it also appears that at a given low value of the Si/Na ratio (see parts E and G of **Figure 6** for Si/Na = 0.1) and therefore with the same distribution of $Q^i$ units, the emulsion with the lowest $Na^+$ concentration is the most stable. At a given Si/Na ratio, the ionic strength increases with the $Na^+$ concentration, possibly altering the chemical equilibrium between

CTA and the silicate species, or destabilizing interfacial and Van der Waals forces through the adsorption of Na+ ions on the droplets. In summary therefore, the stability of these emulsions depends on the interplay of several parameters (the interfacial tension, the degree of polymerization of the silicates, and the ionic strength of the solution), all of which need to be optimized.

## 4. Conclusions

Interactions between silicates and hexadecyltrimethylammonium was studied and published in many articles [63–67]. However, these previous works were focused on the diluted aqueous silicate solutions ([Si] less than 1 $mol.L^{-1}$) and for solutions where the monomer is in the majority.

In this work, the effects of CTAB and silicate oligomers on the stability of emulsions of dodecane and concentrated aqueous silicate solution is highlighted. The interfacial tension decreases from 47 to 20 $mN.m^{-1}$ even in the absence of surfactant, through the cumulative effects of $HO^-$ and silicate groups, with larger silicate oligomers seeming to reduce the interfacial tension the most. However, this decrease is insufficient to obtain a stable emulsion.

Adding DeTAB significantly reduces the interfacial tension but does not lead to a stable emulsion. CTAB also reduces the interfacial tension but leads to the precipitation of CTA-silicate species [65], which contribute to stabilizing the water/oil emulsion, possibly through the Pickering effect. The stability of these emulsions also depends on the interconnectivity of the silicate units and the ionic strength of the alkali silicate solutions. Indeed, the water/oil emulsions formed in the presence of precipitates of mainly monomeric silicates are more stable than those that form when the silicates are mainly oligomers, and the emulsions in higher ionic strength solutions are less stable than those formed when the ionic strength is lower.

**Acknowledgements:** The authors wish to thank Dr. Pierre Bauduin (Institut de Chimie Séparative de Marcoule, Bagnols-sur-Cèze, France) for valuable discussion on the effects of ions. The Chevreul Institute (FR 2638), the Ministère de l'Enseignement Supérieur et de la

Recherche, the Région Nord – Pas de Calais and the FEDER are also acknowledged for supporting and partially funding this work.

## References

[1] J. Davidovits, Geopolymers: inorganic polymeric new materials, Journal of Thermal Analysis and Calorimetry. 37 (1991) 1633–1656.

[2] P. Duxson, A. Fernández-Jiménez, J.L. Provis, G.C. Lukey, A. Palomo, J.S. van Deventer, Geopolymer technology: the current state of the art, Journal of Materials Science. 42 (2007) 2917–2933.

[3] M. Moliner, F. Rey, A. Corma, Towards the Rational Design of Efficient Organic Structure-Directing Agents for Zeolite Synthesis, Angewandte Chemie International Edition. 52 (2013) 13880–13889. https://doi.org/10.1002/anie.201304713.

[4] R. Li, N. Linares, J.G. Sutjianto, A. Chawla, J. Garcia-Martinez, J.D. Rimer, Ultrasmall Zeolite L Crystals Prepared from Highly Interdispersed Alkali-Silicate Precursors, Angewandte Chemie International Edition. 57 (2018) 11283–11288. https://doi.org/10.1002/anie.201805877.

[5] V. Vattipalli, A.M. Paracha, W. Hu, H. Chen, W. Fan, Broadening the Scope for Fluoride-Free Synthesis of Siliceous Zeolites, Angewandte Chemie International Edition. 57 (2018) 3607–3611. https://doi.org/10.1002/anie.201712684.

[6] H. Zhang, A.I. Cooper, Synthesis and applications of emulsion-templated porous materials, Soft Matter. 1 (2005) 107–113.

[7] X.-Y. Yang, L.-H. Chen, Y. Li, J.C. Rooke, C. Sanchez, B.-L. Su, Hierarchically porous materials: synthesis strategies and structure design, Chemical Society Reviews. 46 (2017) 481–558.

[8] A.R. Studart, U.T. Gonzenbach, E. Tervoort, L.J. Gauckler, Processing routes to macroporous ceramics: a review, Journal of the American Ceramic Society. 89 (2006) 1771–1789.

[9] J.L. Provis, P. Duxson, G.C. Lukey, F. Separovic, W.M. Kriven, J.S.J. van Deventer, Modeling Speciation in Highly Concentrated Alkaline Silicate Solutions., Ind. Eng. Chem. Res. 44 (2005) 8899–8908. https://doi.org/10.1021/ie050700i.

[10] D. Medpelli, J.-M. Seo, D.-K. Seo, Geopolymer with Hierarchically Meso-/Macroporous Structures from Reactive Emulsion Templating., J. Am. Ceram. Soc. 97 (2014) 70–73. https://doi.org/10.1111/jace.12724.

[11] L. Salvo, G. Martin, M. Suard, A. Marmottant, R. Dendievel, J.-J. Blandin, Processing and structures of solids foams, Comptes Rendus Physique. 15 (2014) 662–673.

[12] J. Liu, G. Jiang, Y. Liu, J. Di, Y. Wang, Z. Zhao, Q. Sun, C. Xu, J. Gao, A. Duan, others, Hierarchical macro-meso-microporous ZSM-5 zeolite hollow fibers with highly efficient catalytic cracking capability, Scientific Reports. 4 (2014) 7276.

[13] L. Meng, X. Zhang, Y. Tang, K. Su, J. Kong, Hierarchically porous silicon–carbon–nitrogen hybrid materials towards highly efficient and selective adsorption of organic dyes, Scientific Reports. 5 (2015) 7910.

[14] Z. Bhumgara, Polyhipe foam materials as filtration media, Filtration & Separation. 32 (1995) 245–251.

[15] T.-Y. Ma, H. Li, A.-N. Tang, Z.-Y. Yuan, Ordered, mesoporous metal phosphonate materials with microporous crystalline walls for selective separation techniques, Small. 7 (2011) 1827–1837.

[16] C. Bai, G. Franchin, H. Elsayed, A. Conte, P. Colombo, High strength metakaolin-based geopolymer foams with variable macroporous structure., J. Eur. Ceram. Soc. 36 (2016) 4243–4249. https://doi.org/10.1016/j.jeurceramsoc.2016.06.045.

[17] V. Cantarel, D. Lambertin, A. Poulesquen, F. Leroux, G. Renaudin, F. Frizon, Geopolymer assembly by emulsion templating: Emulsion stability and hardening mechanisms., Ceram. Int. 44 (2018) 10558–10568. https://doi.org/10.1016/j.ceramint.2018.03.079.

[18] D. Lambertin, V. Cantarel, A. Poulesquen, F. Frizon, Production of geopolymer composites comprising organic phase change materials., 2018.
[19] S. Trussell, R. Spence, A review of solidification/stabilization interferences, Waste Management. 14 (1994) 507–519.
[20] V. Cantarel, Etude de la synthèse de composites liquides organiques/géopolymère en vue du conditionnement de déchets nucléaires, 2016.
[21] A.H. Demond, A.S. Lindner, Estimation of interfacial tension between organic liquids and water., Environ. Sci. Technol. 27 (1993) 2318–31. https://doi.org/10.1021/es00048a004.
[22] Weissenborn, Pugh, Surface Tension of Aqueous Solutions of Electrolytes: Relationship with Ion Hydration, Oxygen Solubility, and Bubble Coalescence, J Colloid Interface Sci. 184 (1996) 550–63.
[23] Z. Li, B.C.-Y. Lu, Surface tension of aqueous electrolyte solutions at high concentrations - representation and prediction., Chem. Eng. Sci. 56 (2001) 2879–2888. https://doi.org/10.1016/S0009-2509(00)00525-X.
[24] A. Elkamel, T. Al-Sahhaf, A.S. Ahmed, Studying the interactions between an Arabian heavy crude oil and alkaline solutions., Pet. Sci. Technol. 20 (2002) 789–807. https://doi.org/10.1081/LFT-120003713.
[25] Y. Marcus, Surface Tension of Aqueous Electrolytes and Ions., J. Chem. Eng. Data. 55 (2010) 3641–3644. https://doi.org/10.1021/je1002175.
[26] S. Kumar, A. Mandal, Studies on interfacial behavior and wettability change phenomena by ionic and nonionic surfactants in presence of alkalis and salt for enhanced oil recovery., Appl. Surf. Sci. 372 (2016) 42–51. https://doi.org/10.1016/j.apsusc.2016.03.024.
[27] M. Kasmaee, F. Varaminian, P. Khadiv-Parsi, J. Saien, Effects of different surfactants and physical properties on the coalescence of dimethyl disulfide drops with mother phase at the interface of sodium hydroxide aqueous solutions., J. Mol. Liq. 263 (2018) 31–39. https://doi.org/10.1016/j.molliq.2018.04.025.
[28] J. Wen, K. Shi, Q. Sun, Z. Sun, H. Gu, Measurement for Surface Tension of Aqueous Inorganic Salt, Frontiers in Energy Research. 6 (2018). https://doi.org/10.3389/fenrg.2018.00012.
[29] C. Zhao, Y. Jiang, M. Li, T. Cheng, W. Yang, G. Zhou, The effect of NaOH on lowering interfacial tension of oil/alkylbenzene sulfonates solution., RSC Adv. (2018) Ahead of Print. https://doi.org/10.1039/c7ra11287d.
[30] J.H. Burk, Comparison of sodium carbonate, sodium hydroxide, and sodium orthosilicate for EOR., SPE Reservoir Eng. 2 (1987) 9–16. https://doi.org/10.2118/12039-PA.
[31] C.I. Chiwetelu, G.H. Neale, V. Hornof, A.E. George, Recovery of a Saskatchewan heavy oil using alkaline solutions., J. Can. Pet. Technol. 33 (1994) 37–42. https://doi.org/10.2118/94-04-05.
[32] P.H. Krumrine, Sodium silicate in chemical flooding processes for recovery of crude oils., ACS Symp. Ser. 194 (1982) 187–213. https://doi.org/10.1021/bk-1982-0194.ch012.
[33] U. Turksoy, S. Bagci, Improved oil recovery using alkaline solutions in limestone medium., J. Pet. Sci. Eng. 26 (2000) 105–119. https://doi.org/10.1016/S0920-4105(00)00025-5.
[34] R.E. Johnson Jr., R.H. Dettre, The wettability of low-energy liquid surfaces., J. Colloid Interface Sci. 21 (1966) 610–22. https://doi.org/10.1016/0095-8522(66)90021-3.
[35] J. Fu, B. Li, Z. Wang, Estimation of fluid-fluid interfacial tensions of multicomponent mixtures., Chem. Eng. Sci. 41 (1986) 2673–9.
[36] P. Creux, J. Lachaise, A. Graciaa, J.K. Beattie, A.M. Djerdjev, Strong Specific Hydroxide Ion Binding at the Pristine Oil/Water and Air/Water Interfaces., J. Phys. Chem. B. 113 (2009) 14146–14150. https://doi.org/10.1021/jp906978v.
[37] P.J. Kreke, L.J. Magid, J.C. Gee, 1H and 13C NMR Studies of Mixed Counterion, Cetyltrimethylammonium Bromide/Cetyltrimethylammonium Dichlorobenzoate, Surfactant Solutions: The Intercalation of Aromatic Counterions., Langmuir. 12 (1996) 699–705. https://doi.org/10.1021/LA9509662.

[38] W. Wang, B. Gu, L. Liang, W.A. Hamilton, Adsorption and structural arrangement of cetyltrimethylammonium cations at the silica nanoparticle- water interface, The Journal of Physical Chemistry B. 108 (2004) 17477–17483.
[39] G. Perez-Sanchez, S.-C. Chien, J.R.B. Gomes, M.N. D. S. Cordeiro, S.M. Auerbach, P.A. Monson, M. Jorge, Multiscale model for templated synthesis of mesoporous silica: essential role of silica oligomers., Chem. Mater. 28 (2016) 2715–2727. https://doi.org/10.1021/acs.chemmater.6b00348.
[40] Y.S. Lee, D. Surjadi, J.F. Rathman, Effects of Aluminate and Silicate on the Structure of Quaternary Ammonium Surfactant Aggregates., Langmuir. 12 (1996) 6202–6210. https://doi.org/10.1021/LA960054F.
[41] A. Albuquerque, C. Vautier-Giongo, H.O. Pastore, Physical chemistry of nanostructured molecular sieves by the study of phase diagrams: the case of the cetyltrimethylammonium bromide-tetramethylammonium silicate-water system., J. Colloid Interface Sci. 284 (2005) 687–693. https://doi.org/10.1016/j.jcis.2004.10.065.
[42] A. Coste, A. Poulesquen, O. Diat, J.-F. Dufrêche, M. Duvail, Investigation of the Structure of Concentrated NaOH Aqueous Solutions by Combining Molecular Dynamics and Wide-Angle X-ray Scattering, J. Phys. Chem. B. 123 (2019) 5121–5130. https://doi.org/10.1021/acs.jpcb.9b00495.
[43] R. Dupuis, D. Gomes Rodrigues, J.-B. Champenois, R. Pellenq, A. Poulesquen, Time resolved alkali silicate decondensation by sodium hydroxide solution, Journal of Physics: Materials. (2019). http://iopscience.iop.org/10.1088/2515-7639/ab5ce9.
[44] J. Aupoil, J.-B. Champenois, J.-B. d'Espinose de Lacaillerie, A. Poulesquen, Interplay between silicate and hydroxide ions during geopolymerization., Cem. Concr. Res. 115 (2019) 426–432. https://doi.org/10.1016/j.cemconres.2018.09.012.
[45] A.V. McCormick, A.T. Bell, C.J. Radke, Quantitative determination of siliceous species in sodium silicate solutions by silicon-29 NMR spectroscopy., Zeolites. 7 (1987) 183–90. https://doi.org/10.1016/0144-2449(87)90048-0.
[46] D. Wu, V. Hornof, Dynamic interfacial tension in hexadecane/water systems containing ready-made and in-situ-formed surfactants., Chem. Eng. Commun. 172 (1999) 85–106. https://doi.org/10.1080/00986449908912765.
[47] L.R. Pratt, A. Pohorille, Hydrophobic Effects and Modeling of Biophysical Aqueous Solution Interfaces., Chem. Rev. (Washington, DC, U. S.). 102 (2002) 2671–2691. https://doi.org/10.1021/cr000692+.
[48] K.G. Marinova, R.G. Alargova, N.D. Denkov, O.D. Velev, D.N. Petsev, I.B. Ivanov, R.P. Borwankar, Charging of Oil-Water Interfaces Due to Spontaneous Adsorption of Hydroxyl Ions., Langmuir. 12 (1996) 2045–51. https://doi.org/10.1021/LA950928I.
[49] H. Cho, A.R. Felmy, R. Craciun, J.P. Keenum, N. Shah, D.A. Dixon, Solution State Structure Determination of Silicate Oligomers by 29Si NMR Spectroscopy and Molecular Modeling., J. Am. Chem. Soc. 128 (2006) 2324–2335. https://doi.org/10.1021/ja0559202.
[50] B.A. Fleming, Kinetics of reaction between silicic acid and amorphous silica surfaces in NaCl solutions., J. Colloid Interface Sci. 110 (1986) 40–64. https://doi.org/10.1016/0021-9797(86)90351-6.
[51] S. Paredes, M. Tribout, L. Sepulveda, Enthalpies of micellization of the quaternary tetradecyl- and -cetyl ammonium salts., J. Phys. Chem. 88 (1984) 1871–5. https://doi.org/10.1021/j150653a040.
[52] M. Rosen, J. Kunjappu, Dispersion and Aggregation of Solids in Liquid Media by Surfactants, in: Surfactants and Interfacial Phenomena: Fourth Edition, 2012: pp. 368–391. https://doi.org/10.1002/9781118228920.ch9.
[53] M. Lavkush Bhaisare, S. Pandey, M. Shahnawaz Khan, A. Talib, H.-F. Wu, Fluorophotometric determination of critical micelle concentration (CMC) of ionic and non-ionic surfactants with

carbon dots via Stokes shift., Talanta. 132 (2015) 572–578. https://doi.org/10.1016/j.talanta.2014.09.011.
[54] N. Yoshida, K. Matsuoka, Y. Moroi, Micelle formation of n-decyltrimethylammonium perfluorocarboxylates., J. Colloid Interface Sci. 187 (1997) 388–395. https://doi.org/10.1006/jcis.1996.4691.
[55] C. Vautier-Giongo, H.O. Pastore, Micellization of CTAB in the presence of silicate anions and the exchange between bromide and silicate at the micelle surface: A step to understand the formation of mesoporous molecular sieves at extremely low surfactant and silicate concentrations., J. Colloid Interface Sci. 299 (2006) 874–882. https://doi.org/10.1016/j.jcis.2006.02.040.
[56] Y.S. Lee, D. Surjadi, J.F. Rathman, Compositional Effects and Hydrothermal Reorganization of Mesoporous Silicates Synthesized in Surfactant Solutions., Langmuir. 16 (2000) 195–202. https://doi.org/10.1021/la9907937.
[57] W. Tjandra, J. Yao, K.C. Tam, Interaction between Silicates and Ionic Surfactants in Dilute Solution., Langmuir. 22 (2006) 1493–1499. https://doi.org/10.1021/la0521185.
[58] J.K. Beattie, A.M. Djerdjev, The pristine oil/water interface: surfactant-free hydroxide-charged emulsions., Angew. Chem., Int. Ed. 43 (2004) 3568–3571. https://doi.org/10.1002/anie.200453916.
[59] G.V. Franks, A.M. Djerdjev, J.K. Beattie, Absence of Specific Cation or Anion Effects at Low Salt Concentrations on the Charge at the Oil/Water Interface., Langmuir. 21 (2005) 8670–8674. https://doi.org/10.1021/la051379b.
[60] C. Stubenrauch, R. von Klitzing, Disjoining pressure in thin liquid foam and emulsion films-new concepts and perspectives., J. Phys.: Condens. Matter. 15 (2003) R1197–R1232. https://doi.org/10.1088/0953-8984/15/27/201.
[61] J.E. Brady, D.F. Evans, G.G. Warr, F. Grieser, B.W. Ninham, Counterion specificity as the determinant of surfactant aggregation., J. Phys. Chem. 90 (1986) 1853–9. https://doi.org/10.1021/j100400a024.
[62] J.C. Vartuli, K.D. Schmitt, C.T. Kresge, W.J. Roth, M.E. Leonowicz, S.B. McCullen, S.D. Hellring, J.S. Beck, J.L. Schlenker, al. et, Effect of Surfactant/Silica Molar Ratios on the Formation of Mesoporous Molecular Sieves: Inorganic Mimicry of Surfactant Liquid-Crystal Phases and Mechanistic Implications., Chem. Mater. 6 (1994) 2317–26. https://doi.org/10.1021/cm00048a018.
[63] J. Vartuli, K. Schmitt, C. Kresge, W. Roth, M. Leonowicz, S. McCullen, S. Hellring, J. Beck, J. Schlenker, Effect of surfactant/silica molar ratios on the formation of mesoporous molecular sieves: inorganic mimicry of surfactant liquid-crystal phases and mechanistic implications, Chemistry of Materials. 6 (1994) 2317–2326.
[64] Y.S. Lee, D. Surjadi, J.F. Rathman, Effects of aluminate and silicate on the structure of quaternary ammonium surfactant aggregates, Langmuir. 12 (1996) 6202–6210. https://doi.org/10.1021/la960054f.
[65] A. Albuquerque, C. Vautier-Giongo, H. Pastore, Physical chemistry of nanostructured molecular sieves by the study of phase diagrams: the case of the cetyltrimethylammonium bromide–tetramethylammonium silicate–water system, Journal of Colloid and Interface Science. 284 (2005) 687–693.
[66] C. Vautier-Giongo, H.O. Pastore, Micellization of CTAB in the presence of silicate anions and the exchange between bromide and silicate at the micelle surface: A step to understand the formation of mesoporous molecular sieves at extremely low surfactant and silicate concentrations, Journal of Colloid and Interface Science. 299 (2006) 874–882.
[67] G. Pérez-Sánchez, S.-C. Chien, J.R. Gomes, M.N. DS Cordeiro, S.M. Auerbach, P.A. Monson, M. Jorge, Multiscale model for the templated synthesis of mesoporous silica: the essential role of silica oligomers, Chemistry of Materials. 28 (2016) 2715–2727.

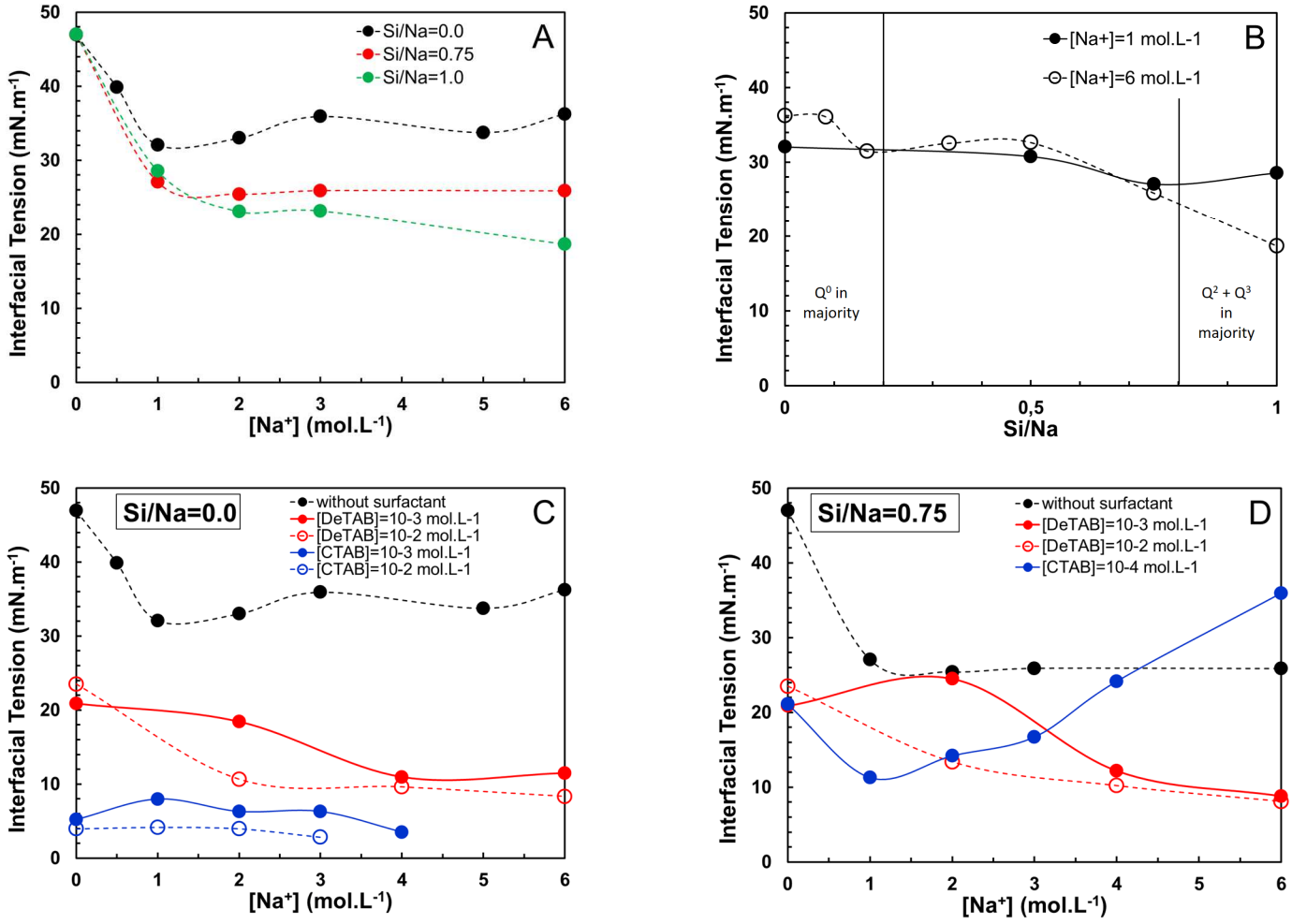


**Figure 1.** Interfacial tension between dodecane and the aqueous phase **(A)** as a function of the $Na^+$ concentration in water with different Si/Na molar ratios (0, 0.75 and 1); (**B**) as a function of the Si/Na molar ratio for $[Na^+]$ = 1 and 6 $mol.L^{-1}$ (the vertical lines delimit areas where more than 70% of the silicon atoms are in the indicated $Q^n$ configuration, according to reference [9]); (**C**) as a function of the Si/Na molar ratio for Si/Na = 0, without surfactant and with either CTAB or DeTAB at $10^{-3}$ and $10^{-2}$ $mol.L^{-1}$; and (**D**) as a function of the Si/Na molar ratio for Si/Na = 0.75, without surfactant and with either CTAB at $10^{-4}$ $mol.L^{-1}$ or DeTAB at $10^{-3}$ and $10^{-2}$ $mol.L^{-1}$. Measurements at [Na+] = 0 $mol.L^{-1}$ in parts **A**, **B** and **C**, where the Si/Na ratio is undefined, were performed in pure water (without or with surfactant).

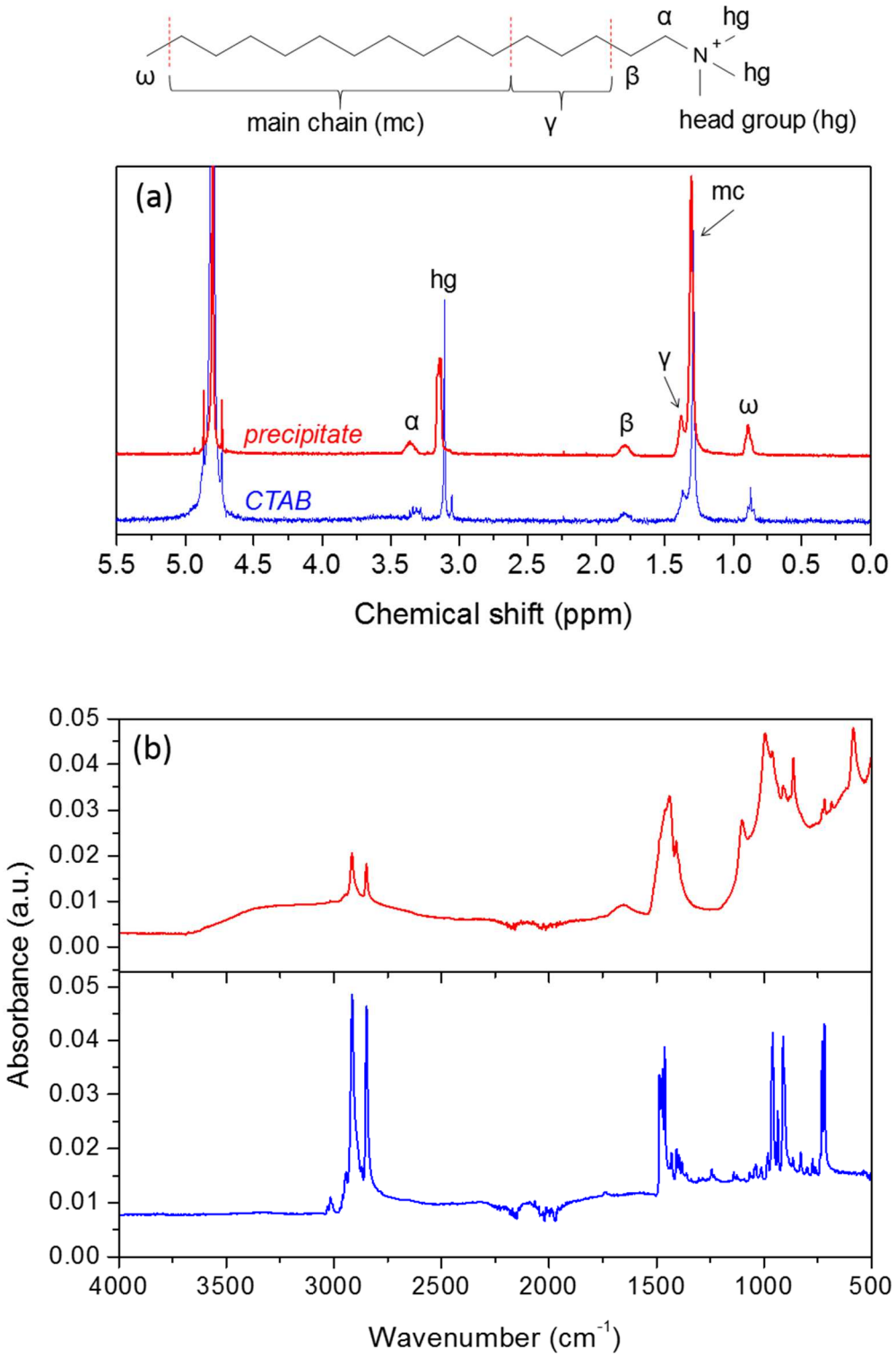


**Figure 2.** (a) $^{1}$H NMR and (b) FTIR spectra of the silicate-CTAB precipitates in comparison with the spectrum of pure CTAB.

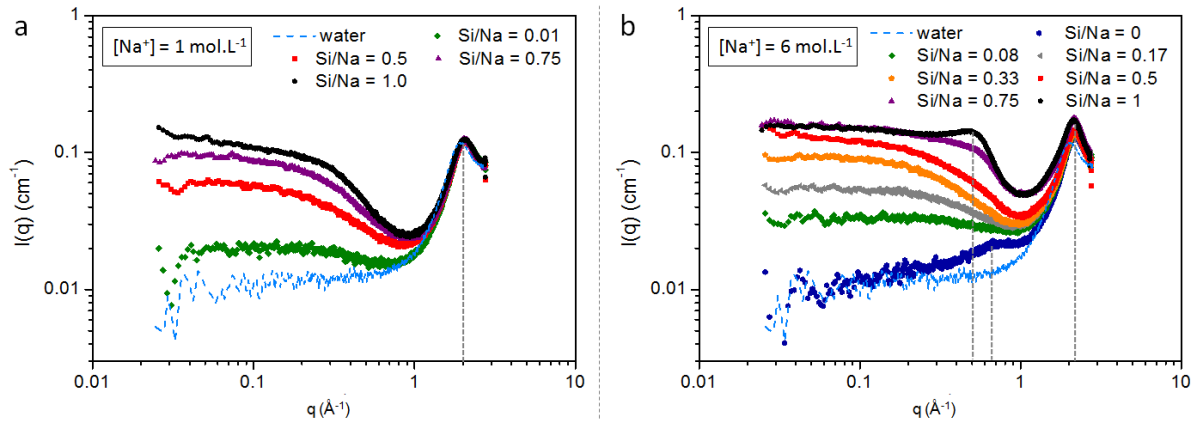


**Figure 3.** SWAXS spectra (I(q) in $cm^{-1}$ *versus* q($Å^{-1}$)) of pure water (dashed lines) and alkali silicate solutions (solid symbols) with various Si/Na molar ratios for (a) $[Na^+]$ = 1 mol·$L^{-1}$ and (b) $[Na^+]$ = 6 mol·$L^{-.1}$.

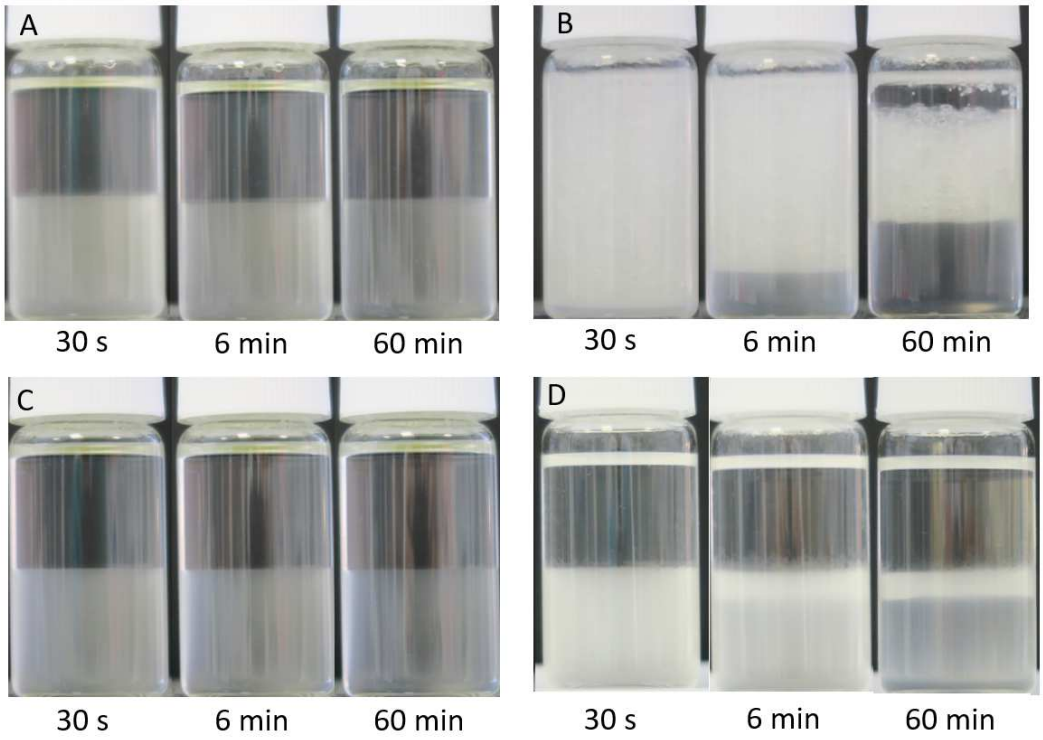


**Figure 4.** Photographs of emulsions 30 s, 6 min and 60 min after mixing 10 mL of dodecane and 10 mL of an aqueous silicate solution ([NaOH] = 6 mol.L$^{-1}$ and [$SiO_2$] = 4.5 mol.L$^{-1}$) with an Ultra-Turrax homogenizer at 13,500 rpm for 60 s. A: aqueous silicate solution, B: aqueous silicate solution + [CTAB] = $10^{-2}$ mol.L$^{-1}$ with the precipitate, C: aqueous silicate solution + [CTAB]=$10^{-2}$ mol.L$^{-1}$ after filtration and removal of the precipitate, D: aqueous silicate solution + [DeTAB]=$10^{-2}$ mol.L$^{-1}$

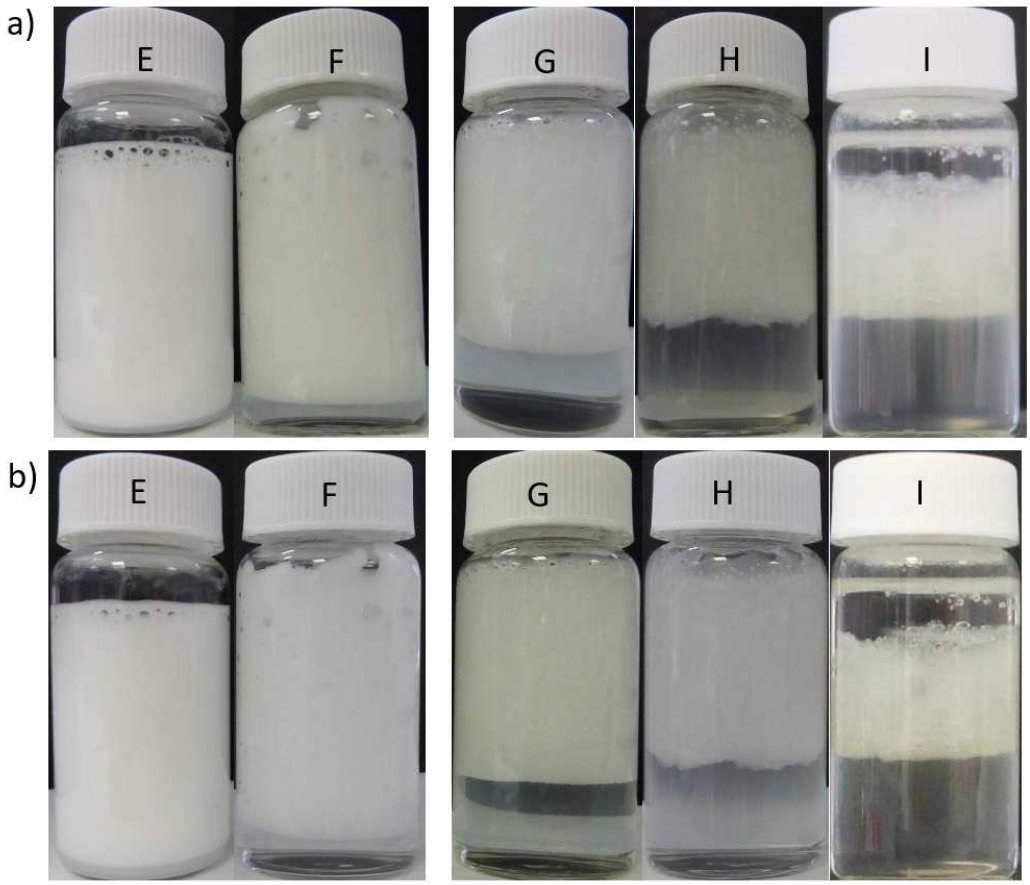


**Figure 5.** Photographs of emulsions (a) 60 and (b) 120 min after mixing 10 mL of dodecane and 10 mL of various aqueous silicate solutions containing $10^{-2}$ mol.L$^{-1}$ CTAB with an Ultra-Turrax homogenizer at 13,500 rpm for 60 s. The compositions of the aqueous silicate solutions are as follows : E: [NaOH]=1 mol.L$^{-1}$ and Si/Na = 0.1, F: [NaOH]=1 mol.L$^{-1}$ and Si/Na = 0.33, G: [NaOH]=6 mol.L$^{-1}$ and Si/Na = 0.1, H: G: [NaOH]=6 mol.L$^{-1}$ and Si/Na = 0.33 and I: G: [NaOH]=6 mol.L$^{-1}$ and Si/Na = 0.75

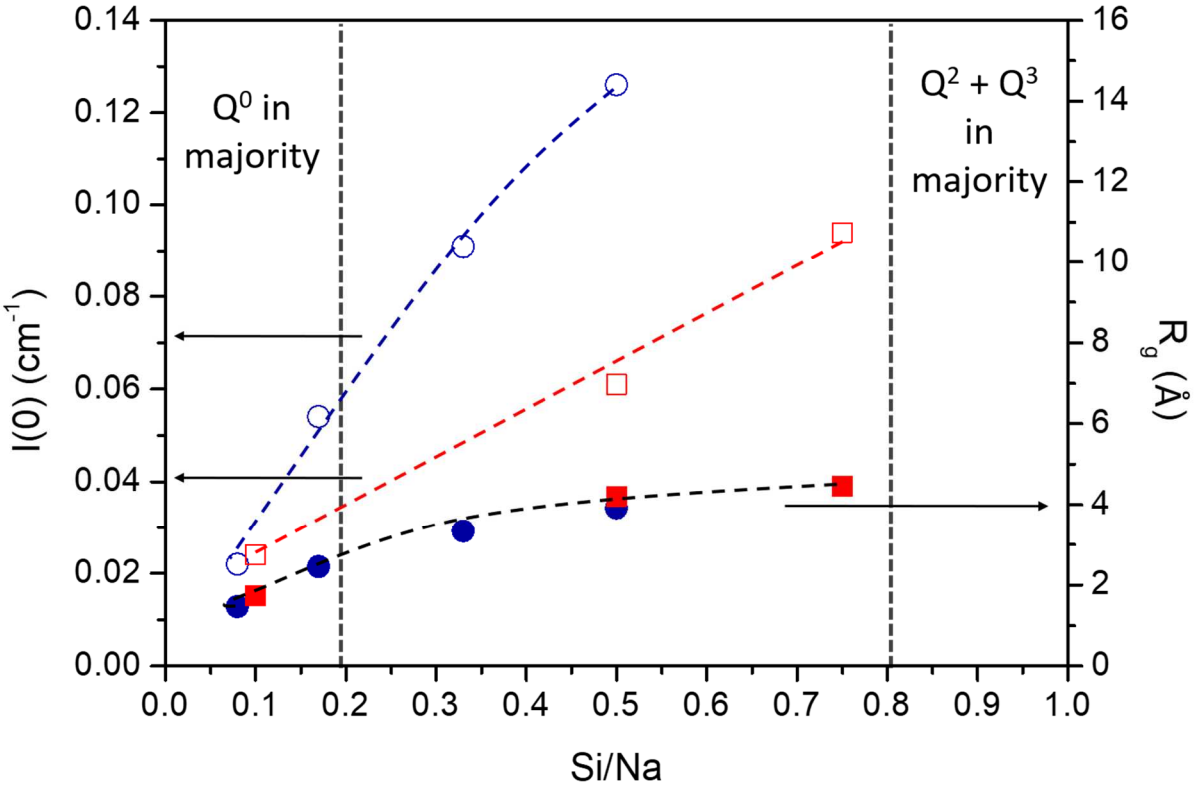


**Figure 6.** Scattering $I_0$ ($cm^{-1}$) and gyration radius of silicate species, $R_g$ (Å), as a function of the Si/Na molar ratio for $[Na^+]$ = 1 (red) and 6 $mol.L^{-1}$(blue). The vertical lines delimit areas where more than 70% of the silicon atoms are in the indicated $Q^n$ configuration, according to reference [9].

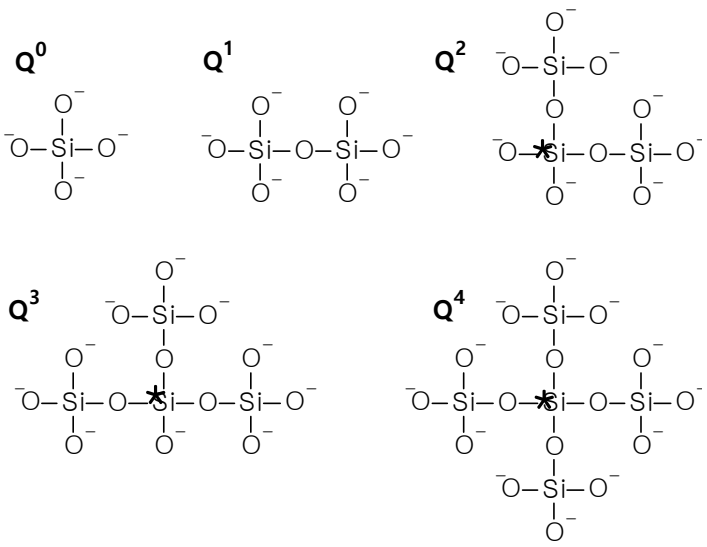


**Figure 7.** Schematic representation of the different silicon centers ($Q^0$, $Q^1$, $Q^2$, $Q^3$, $Q^4$) indicated by an asterisk. For clarity, the oxygen atoms are represented as fully ionized.

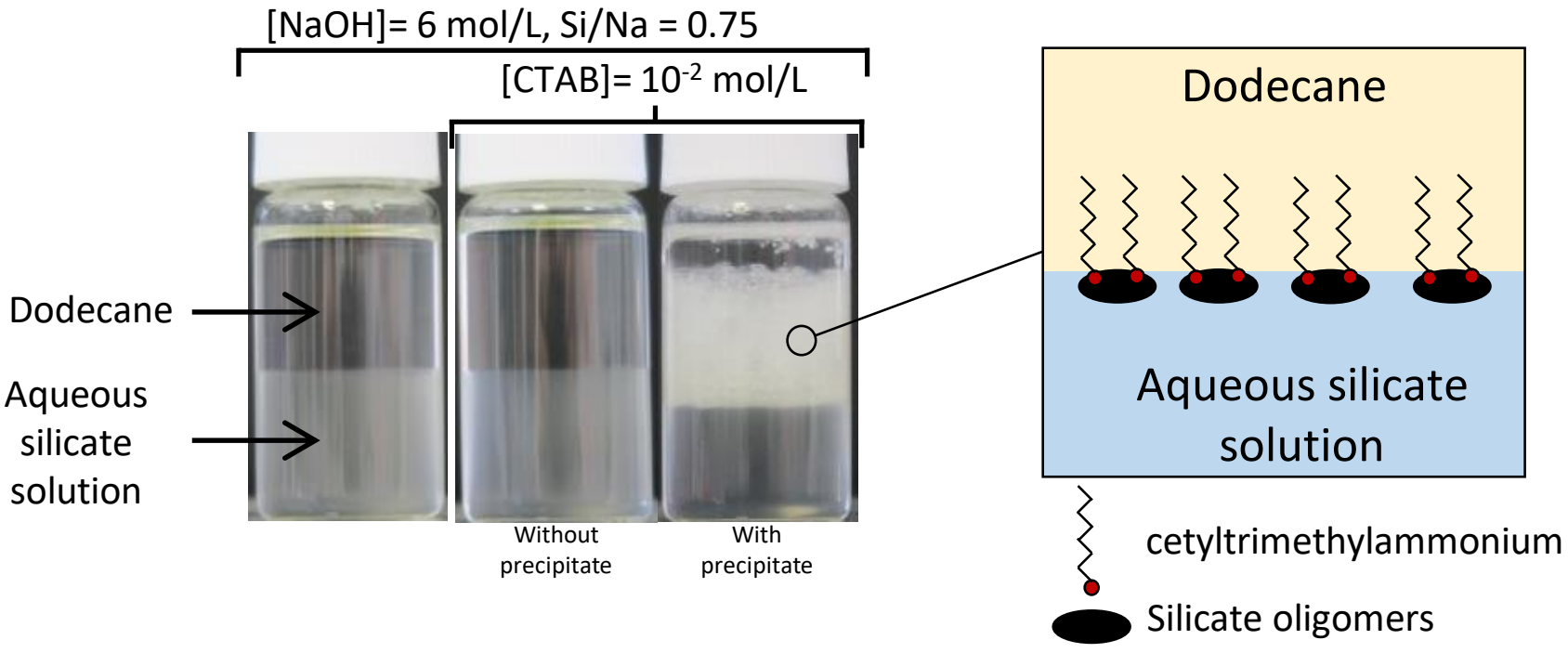
[NaOH]= 6 mol/L, Si/Na = 0.75
[CTAB]= 10-2 mol/L
Dodecane
Aqueous silicate solution
Without precipitate
With precipitate
Dodecane
Aqueous silicate solution
cetyltrimethylammonium
Silicate oligomers